



Gas-Phase Ozonolysis of Furan, Methylfurans, and Dimethylfurans in the Atmosphere

Mengke Li,^a Yuhong Liu^a and Liming Wang ^{*a,b}

^a School of Chemistry & Chemical Engineering, South China University of Technology, Guangzhou 510640, China. Email: wanglm@scut.edu.cn

^b Guangdong Provincial Key Laboratory of Atmospheric Environment and Pollution Control, South China University of Technology, Guangzhou 510006, China.

Electronic Supplementary Information: Figure S1-S11

Figure S1. Structures at M06-2X/6-311++G(2df,2p) level

Figure S2. CASSCF(8,6)/6-311+G(d) calculation on CH₂=CHCHO

Figure S3. The profiles of fractional yield of product channels in the ozonolysis of furan at 298 K and 760 Torr, obtained from RRKM-ME calculations based on F12/VTZ energies

Figure S4. Potential energy diagram for reaction between 2,5-DMF and O₃ at CCSD(T)-F12a level with cc-pVDZ-F12 [cc-pVTZ-F12] basis set

Figure S5. Interconversions and isomerizations of 2,5-DMF-CI1-*syn* at RHF-CCSD(T)-F12a/cc-pVDZ-F12 level. Energies are relative to separate 2,5-DMF and O₃

Figure S6. The profiles of fractional yield of product channels in the ozonolysis of 2,5-DMF at 298 K and 760 Torr, obtained from RRKM-ME calculations based on F12/VDZ energies

Figure S7. Interconversions and isomerizations of 3-MF-CI1-*syn* and 3-MF-CI3-*syn* at RHF-CCSD(T)-F12a/cc-pVDZ-F12 level. Energies are relative to separate 2,3-DMF and O₃

Figure S8. Potential energy diagrams for reaction between 2-methylfuran and O₃ at levels of CCSD(T)-F12a/cc-pVDZ-F12 [and CCSD(T)-F12a/cc-pVTZ-F12]

Figure S9. Interconversions and isomerizations of 3-MF-CI1-*syn* and 3-MF-CI3-*syn* at RHF-CCSD(T)-F12a/cc-pVDZ-F12 level. Energies are relative to separate 2,3-DMF and O₃

Figure S10. Potential energy diagrams for reaction between 2,3-dimethylfuran and O₃ at levels of CCSD(T)-F12a/cc-pVDZ-F12 [and CCSD(T)-F12a/cc-pVTZ-F12]

Figure S11. Interconversions and isomerizations of 2,3-DMF-CI1-*syn* and 2,3-DMF-CI3-*syn* at RHF-CCSD(T)-F12a/cc-pVDZ-F12 level. Energies are relative to separate 2,3-DMF and O₃

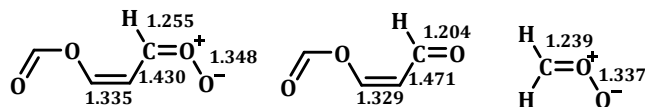


Figure S1. Structures at M06-2X/6-311++G(2df,2p) level (bond lengths in Ångström).

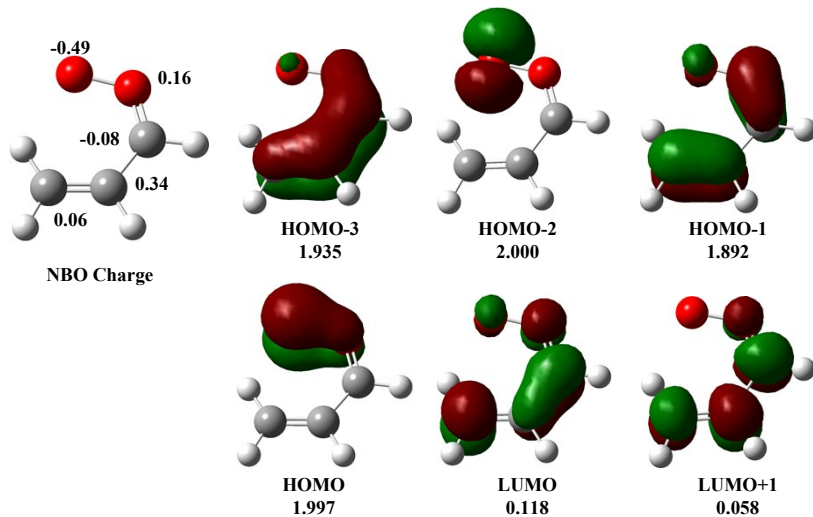


Figure S2. CASSCF(8,6)/6-311+G(d) calculation on $\text{CH}_2=\text{CHCHO}$: the NBO charges, the active orbitals and their orbital occupancies.

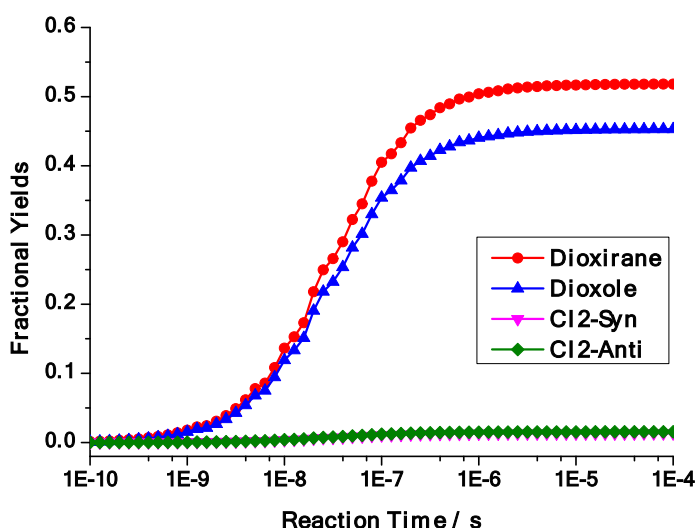


Figure S3. The profiles of fractional yield of product channels in the ozonolysis of furan at 298 K and 760 Torr, obtained from RRKM-ME calculations based on F12/VTZ energies.

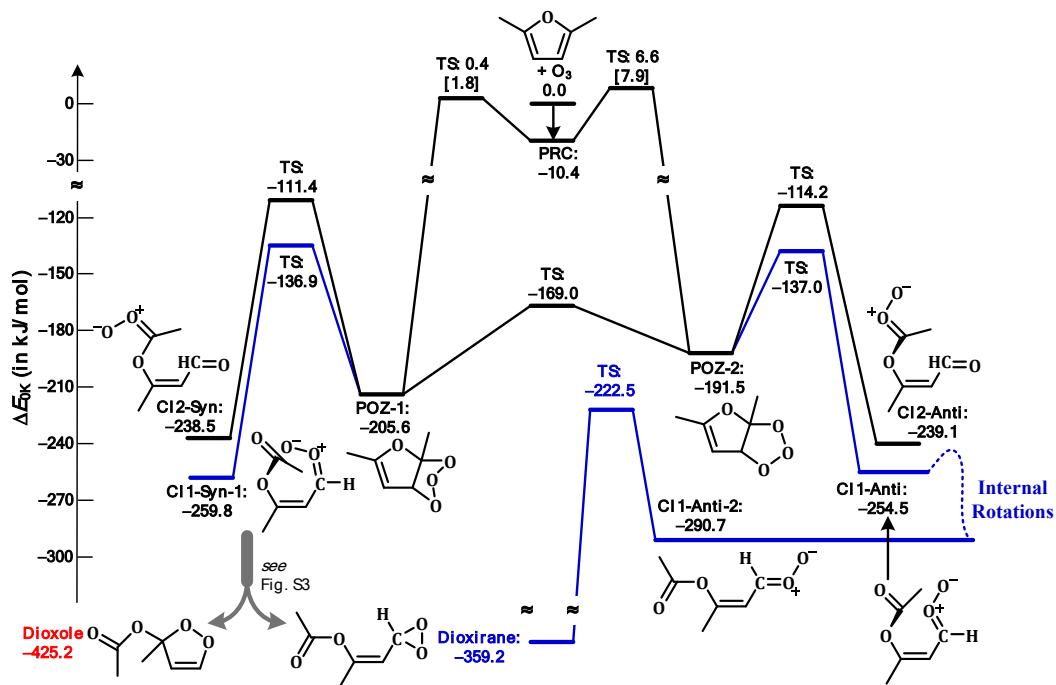


Figure S4. Potential energy diagram for reaction between 2,5-DMF and O_3 at CCSD(T)-F12a level with cc-pVDZ-F12 [cc-pVTZ-F12] basis set.

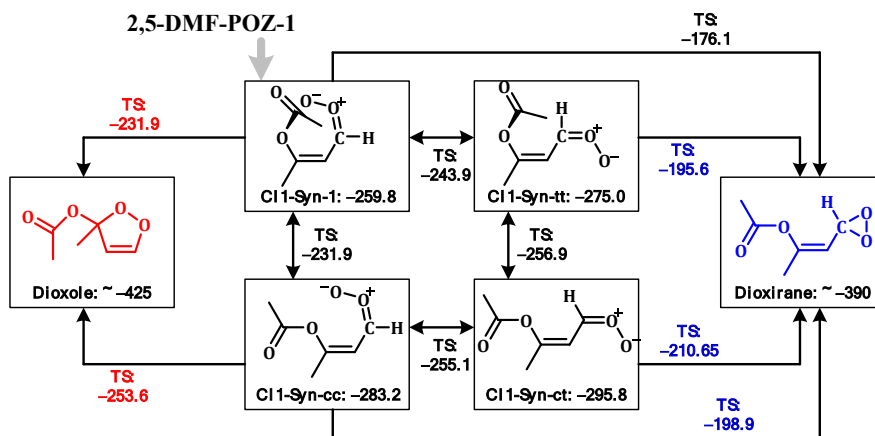


Figure S5. Interconversions and isomerizations of 2,5-DMF-CI1-*syn* at RHF-CCSD(T)-F12a/cc-pVDZ-F12 level. Energies are relative to separate 2,5-DMF and O_3 .

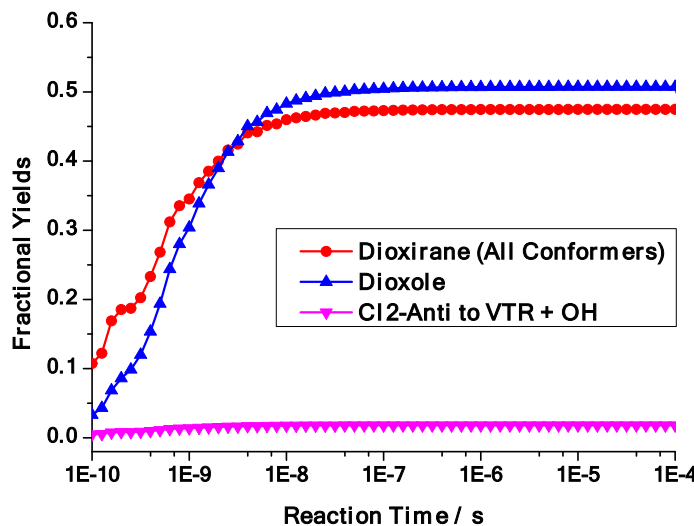


Figure S6. The profiles of fractional yield of product channels in the ozonolysis of 2,5-DMF at 298 K and 760 Torr, obtained from RRKM-ME calculations based on F12/VDZ energies.

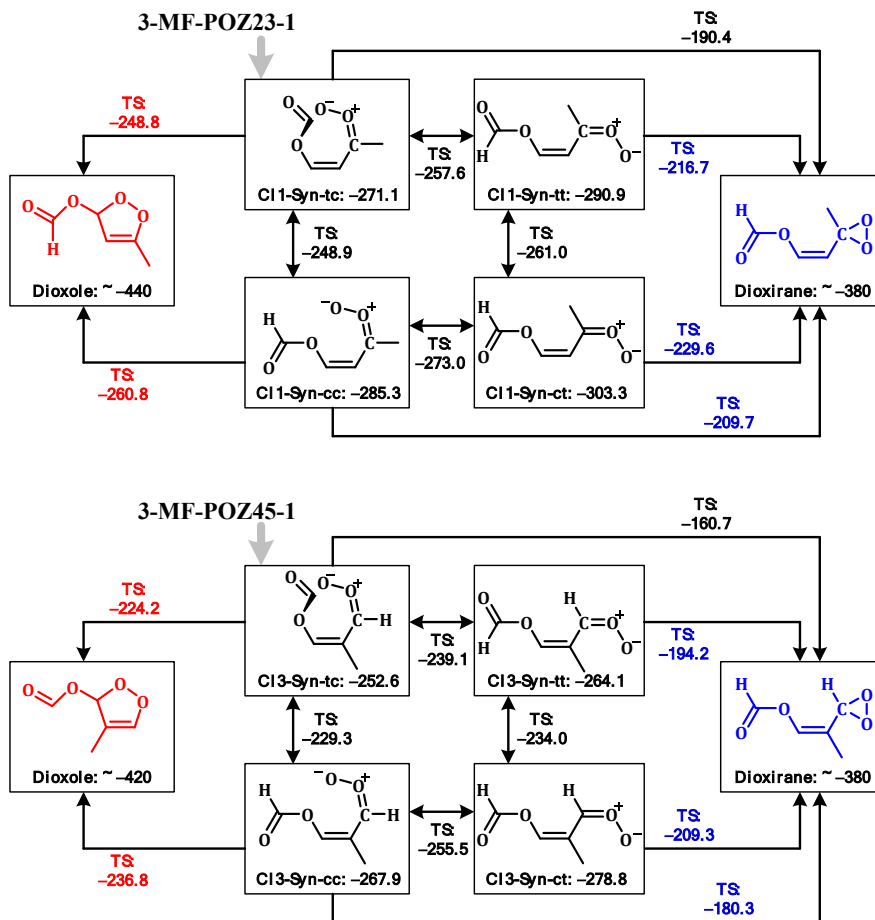


Figure S7. Interconversions and isomerizations of 3-MF-CI1-*syn* and 3-MF-CI3-*syn* at RHF-CCSD(T)-F12a/cc-pVDZ-F12 level. Energies are relative to separate 2,3-DMF and O₃.

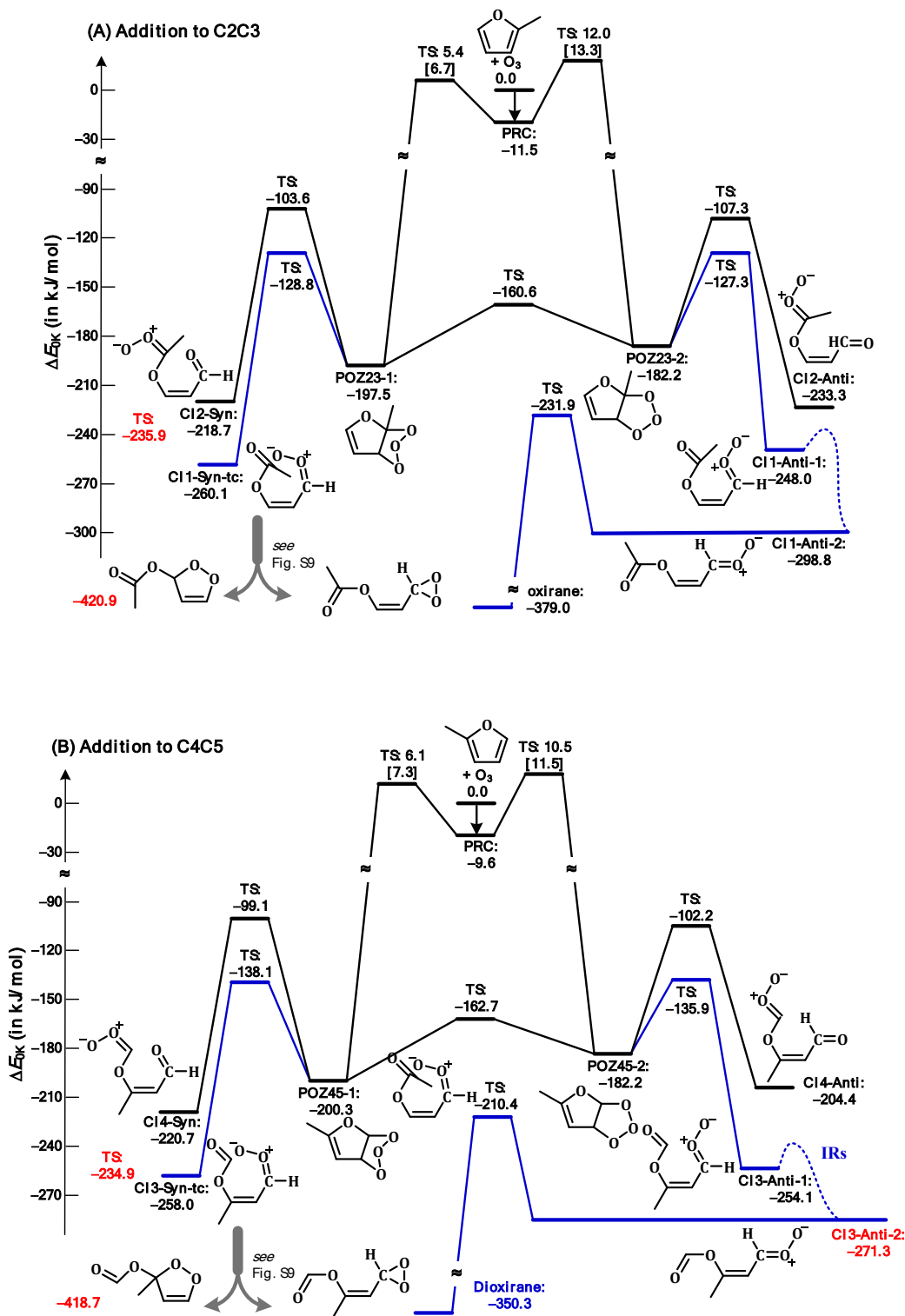


Figure S8. Potential energy diagrams for reaction between 2-methylfuran and O_3 at levels of CCSD(T)-F12a/cc-pVDZ-F12 [and CCSD(T)-F12a/cc-pVTZ-F12]

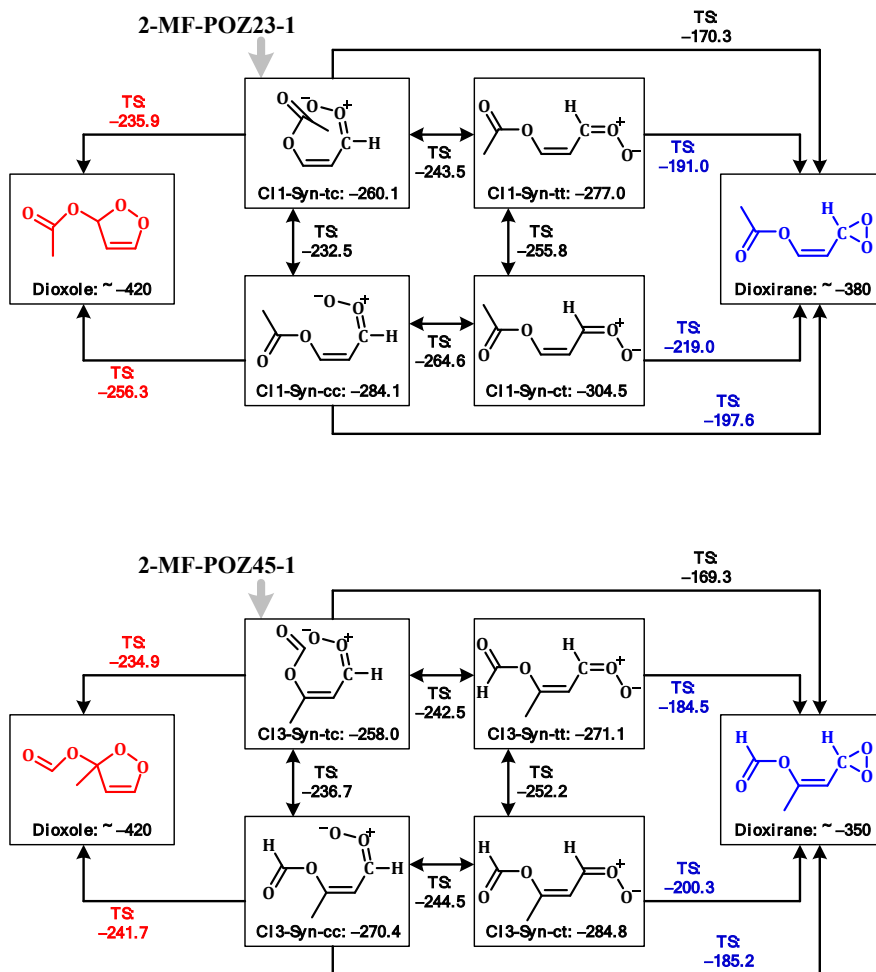


Figure S9. Interconversions and isomerizations of 3-MF-CI1-*syn* and 3-MF-CI3-*syn* at RHF-CCSD(T)-F12a/cc-pVDZ-F12 level. Energies are relative to separate 2,3-DMF and O₃.

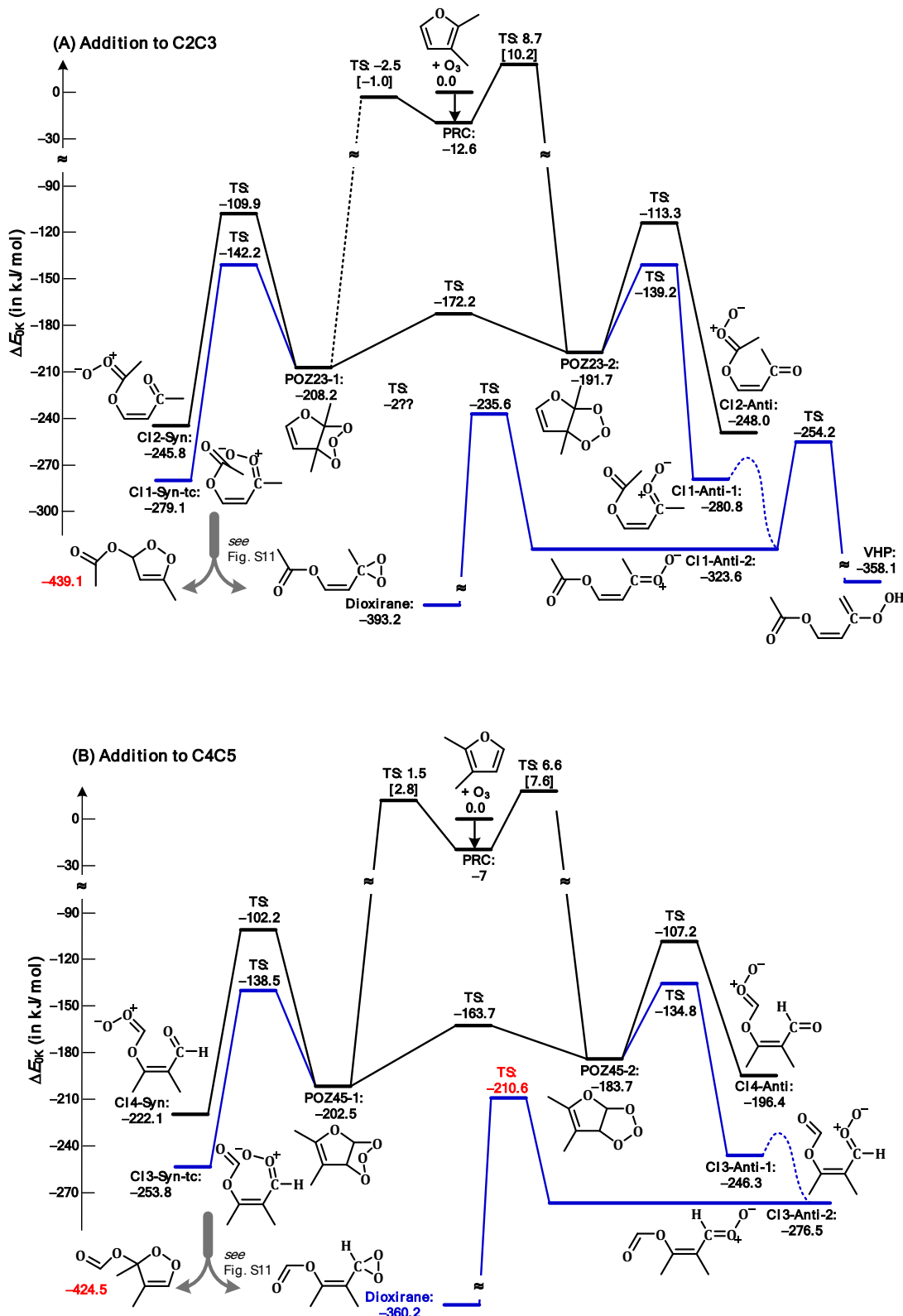


Figure S10. Potential energy diagrams for reaction between 2,3-dimethylfuran and O_3 at levels of CCSD(T)-F12a/cc-pVDZ-F12 [and CCSD(T)-F12a/cc-pVTZ-F12]

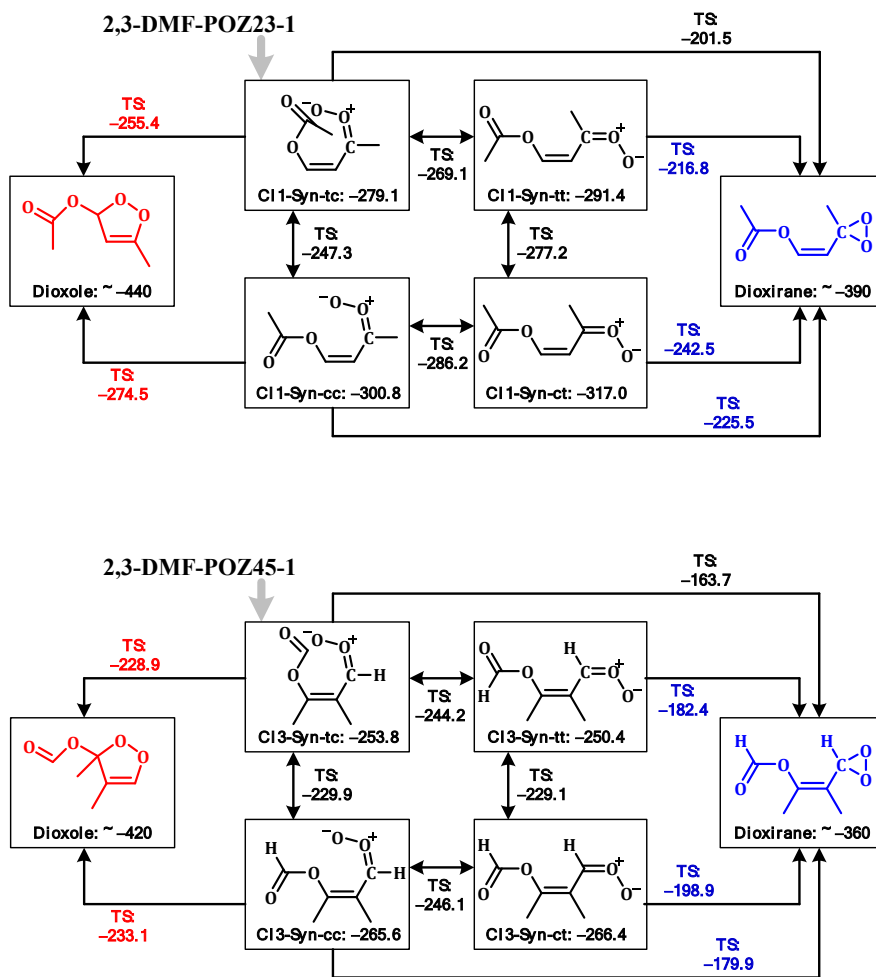


Figure S11. Interconversions and isomerizations of 2,3-DMF-CI1-*syn* and 2,3-DMF-CI3-*syn* at RHF-CCSD(T)-F12a/cc-pVDZ-F12 level. Energies are relative to separate 2,3-DMF and O₃.